

Supporting Information

Callistemon-like Zn and S codoped CoP nanorod clusters as highly efficient electrocatalysts for neutral-pH overall water splitting

Liang Yan, Bing Zhang, Junlu Zhu, Zhonggang Liu, Haiyan Zhang and Yunyong Li^{*}

Guangdong Provincial Key Laboratory of Functional Soft Condensed Matter, School of Materials and Energy, Guangdong University of Technology, No. 100 Waihuan Xi Road, Guangzhou Higher Education Mega Center, Guangzhou, 510006, China

**Corresponding author.*

E-mail address: yyli@gdut.edu.cn (Y. Li)

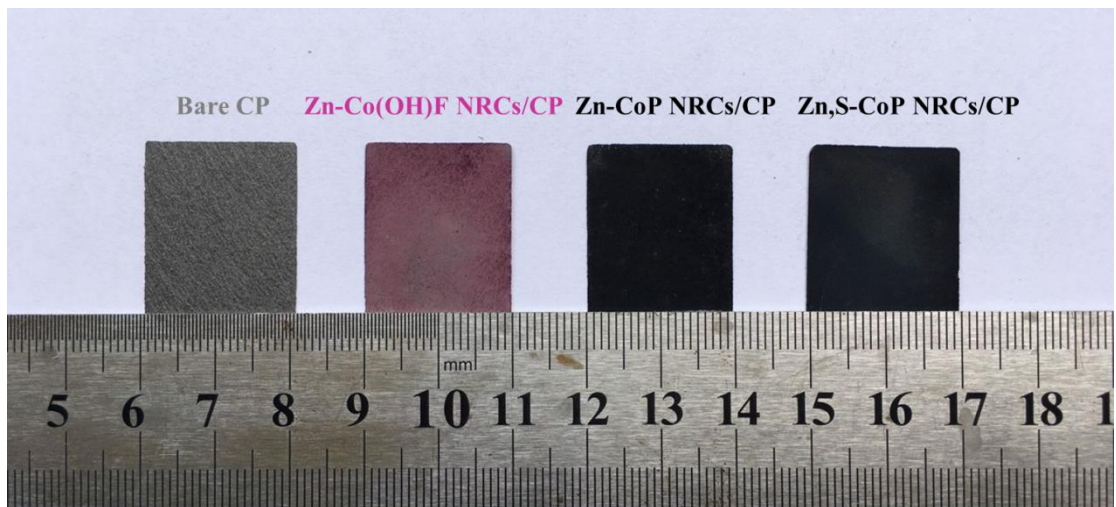


Figure S1. Optical photographs of bare CP, Zn-Co(OH)F NRCs/CP, Zn-CoP NRCs/CP, and Zn,S-CoP NRCs/CP.

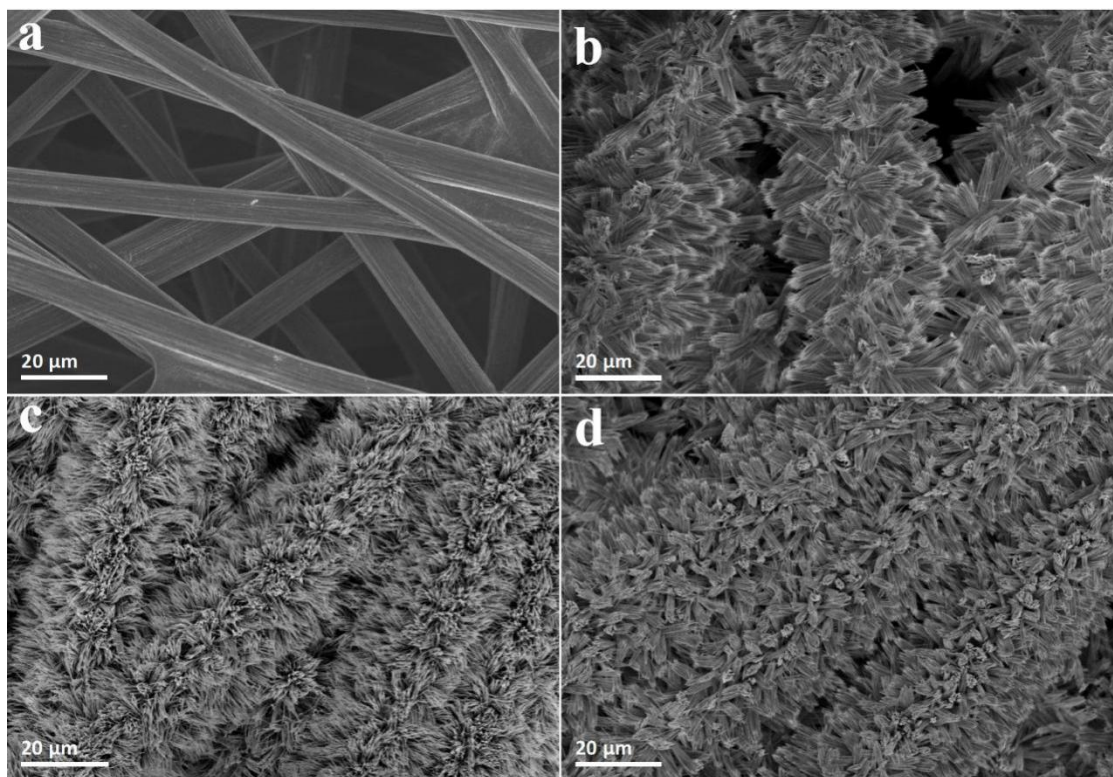


Figure S2. SEM images of (a) bare CP, (b) Zn-Co(OH)F NRCs/CP, (c) Zn-CoP NRCs/CP, and (d) Zn,S-CoP NRCs/CP.

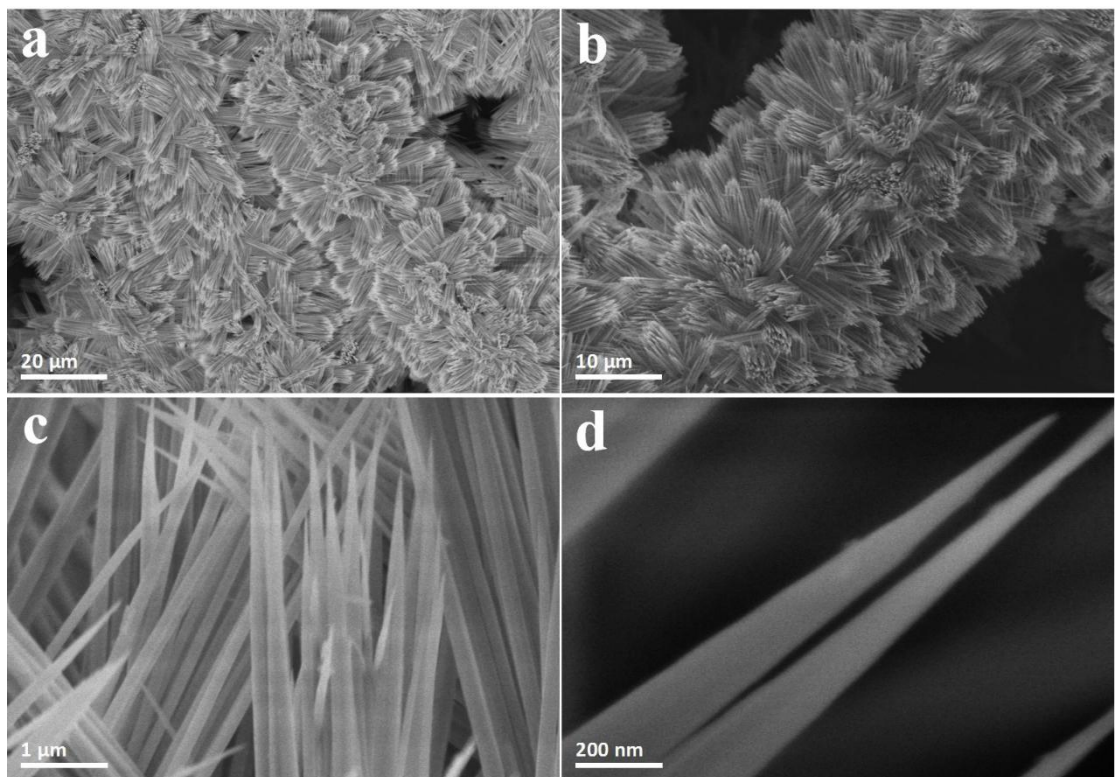


Figure S3. (a,b) Low-magnification and (c,d) high-magnification SEM images of Zn-Co(OH)F NRCs/CP.

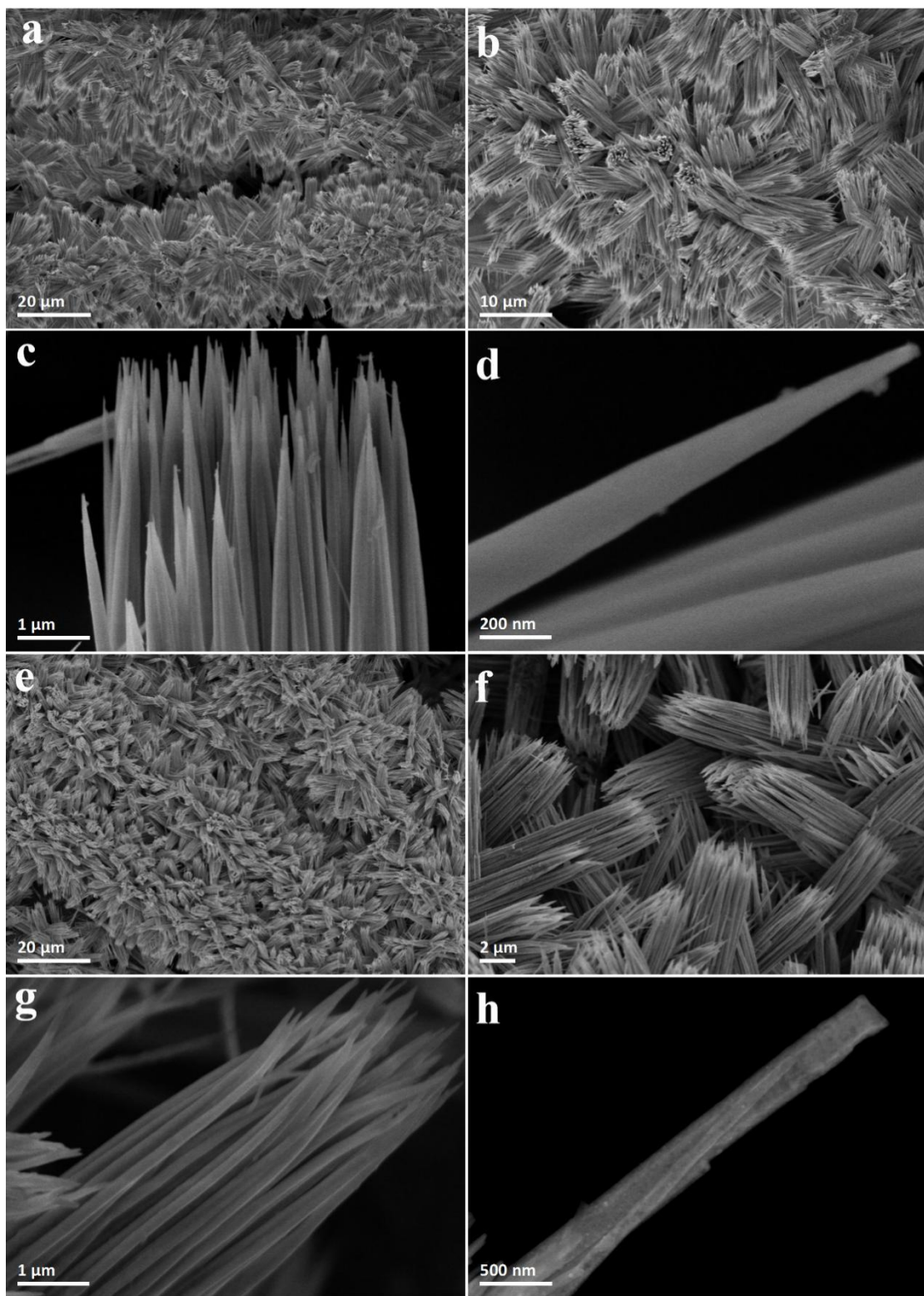


Figure S4. (a,b) Low-magnification and (c,d) high-magnification SEM images of Co(OH)F NRCs/CP. (e,f) Low-magnification and (g,h) high-magnification SEM images of CoP NRCs/CP.

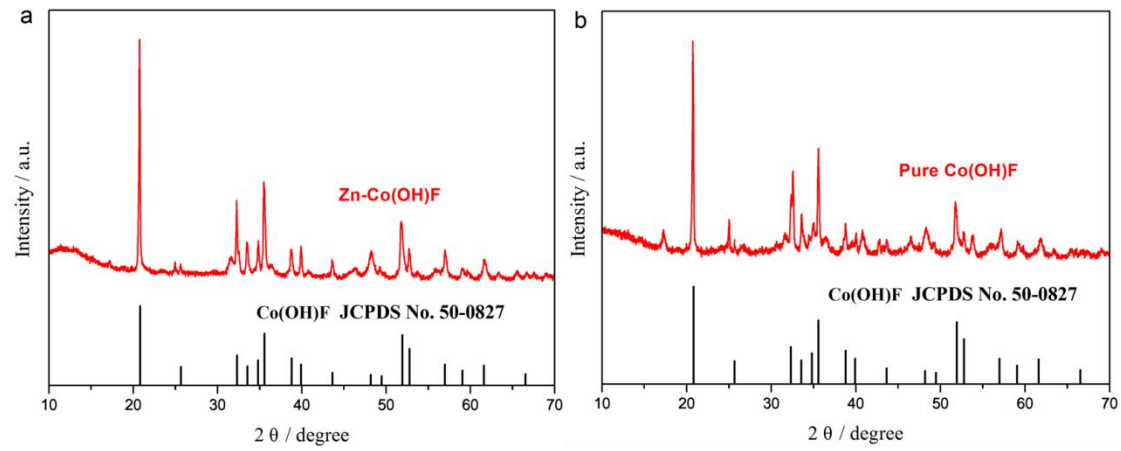


Figure S5. XRD patterns of (a) Zn-Co(OH)F NRCs and (b) pure Co(OH)F NRCs.

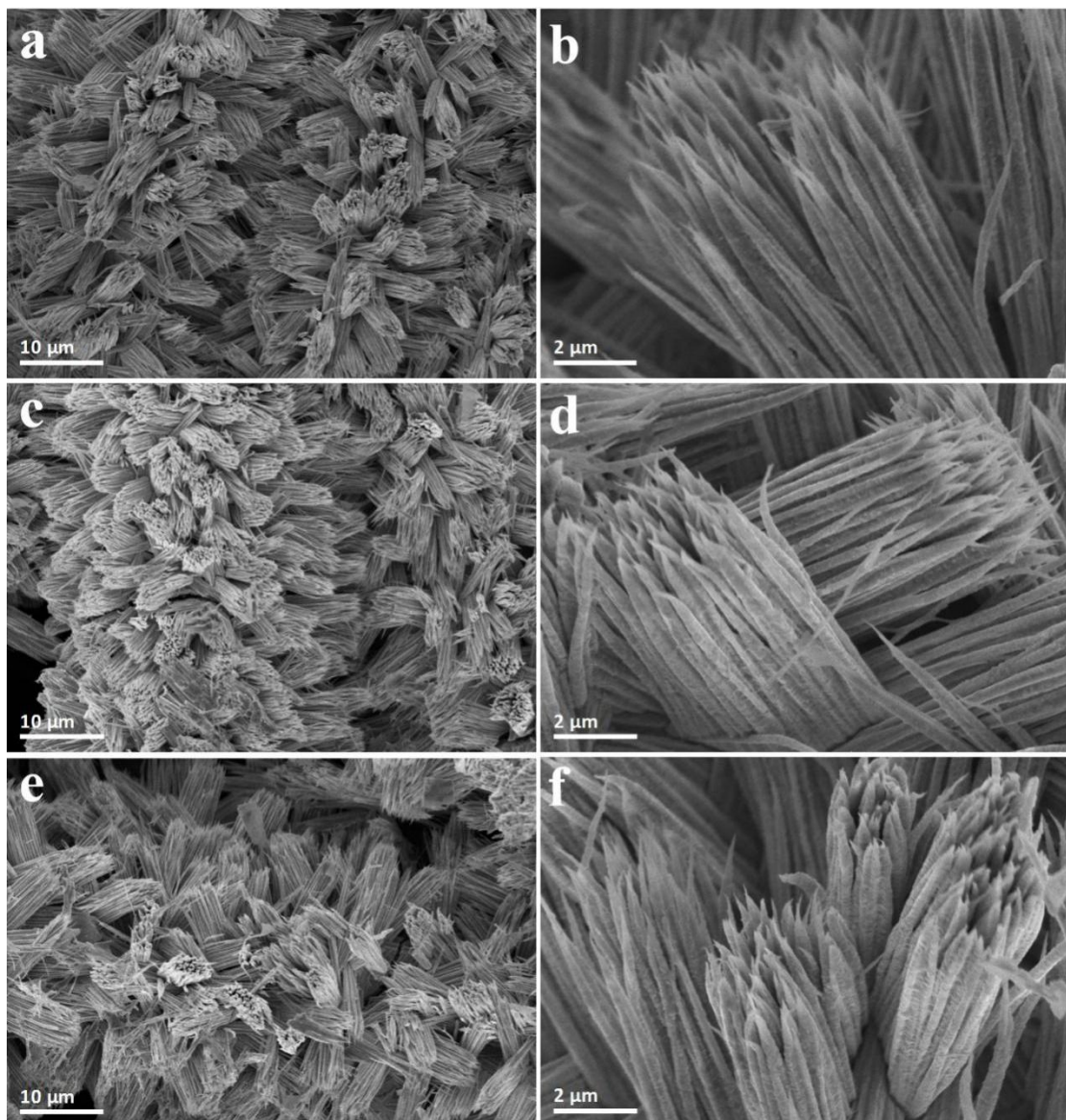


Figure S6. SEM images of (a,b) $\text{Zn}_{0.025}\text{S}-\text{Co}_{0.975}\text{P}$ NRCs/CP, (c,d) $\text{Zn}_{0.05}\text{S}-\text{Co}_{0.95}\text{P}$ NRCs/CP, and (e,f) $\text{Zn}_{0.1}\text{S}-\text{Co}_{0.9}\text{P}$ NRCs/CP.

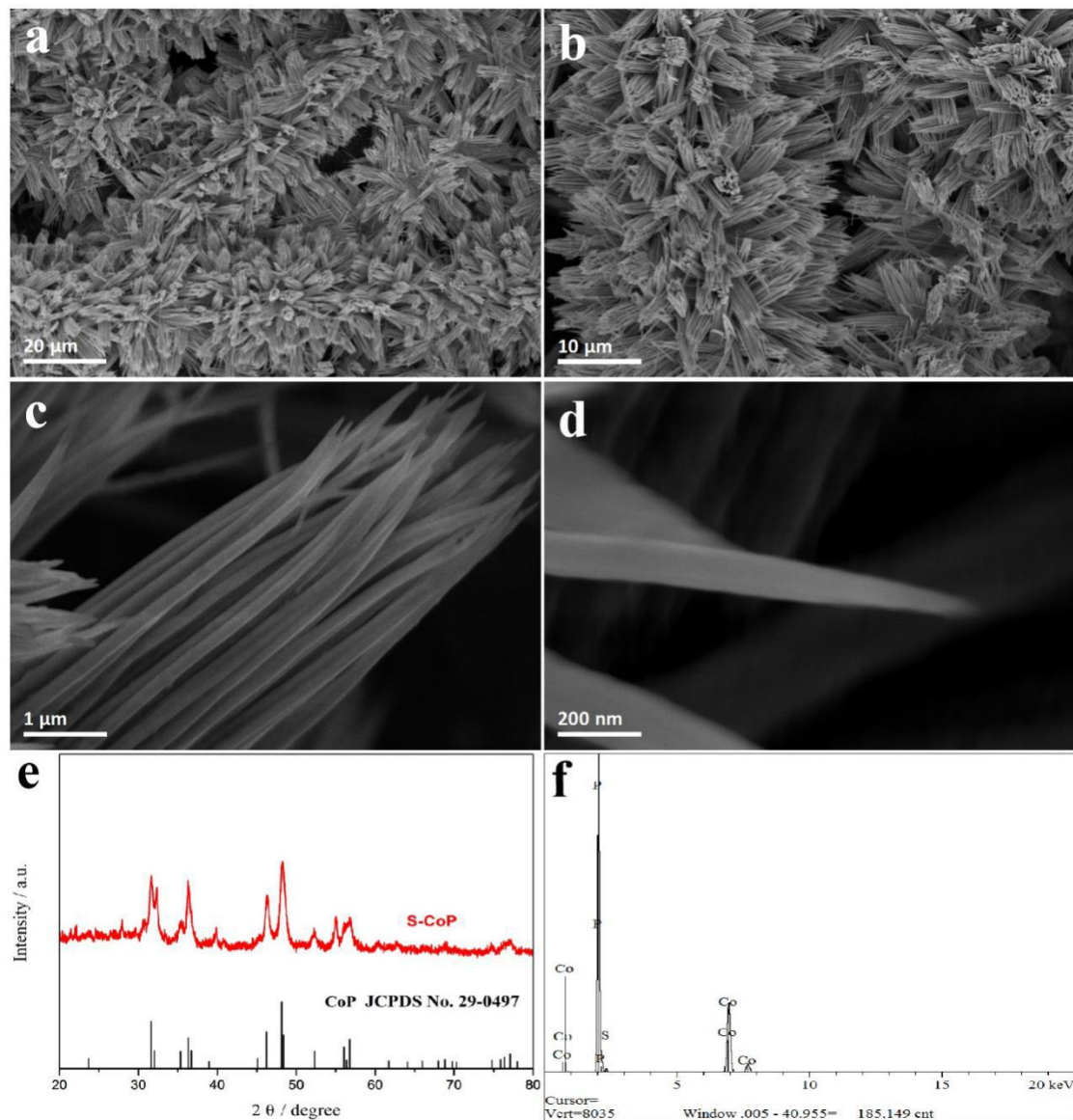


Figure S7. (a,b) Low-magnification and (c,d) high-magnification SEM images, (e) XRD pattern, and (f) EDX pattern of S-CoP NRCs/CP.

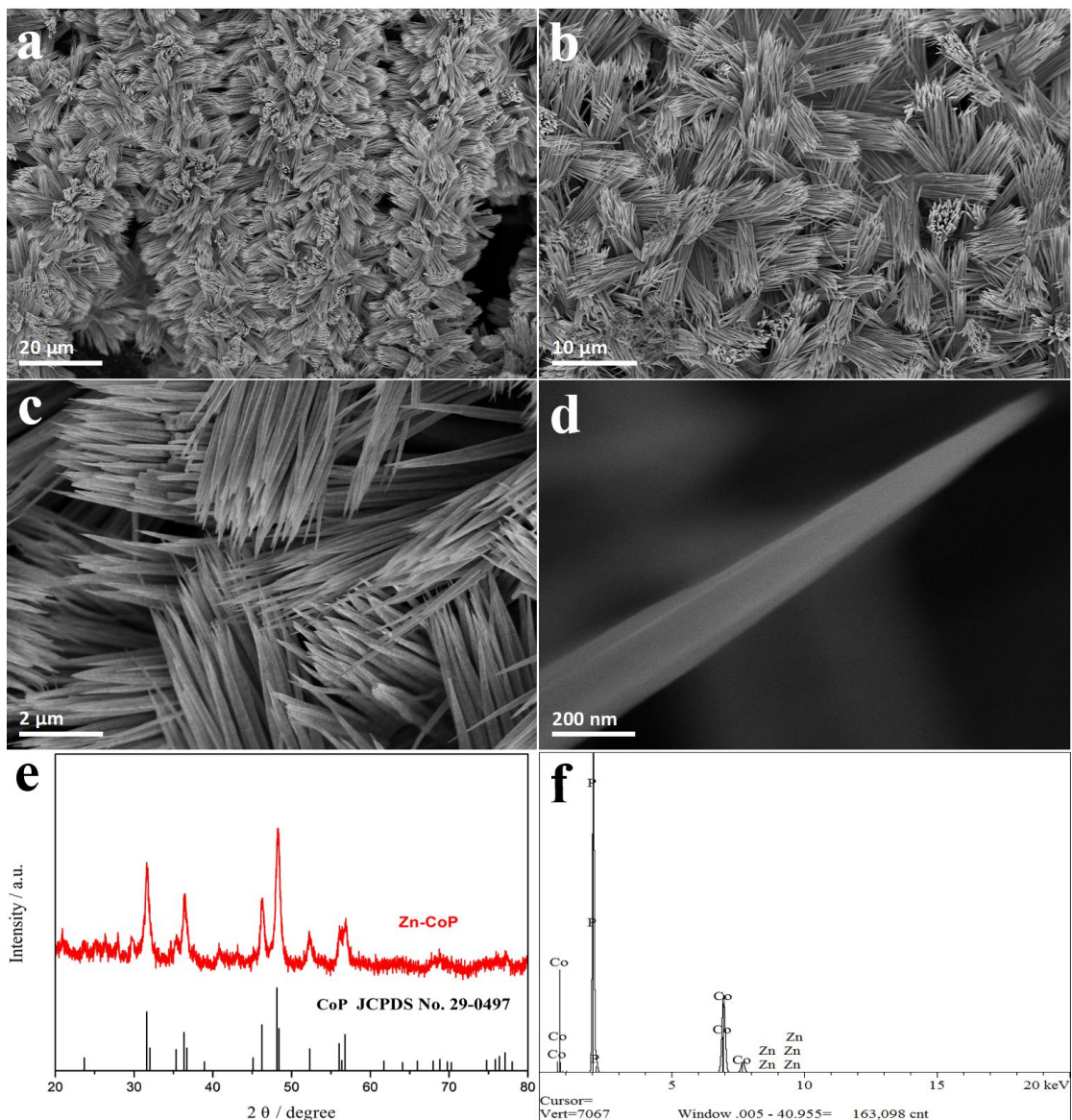


Figure S8. (a,b) Low-magnification and (c,d) high-magnification SEM images, (e) XRD pattern, and (f) EDX pattern of Zn-CoP NRCs/CP.

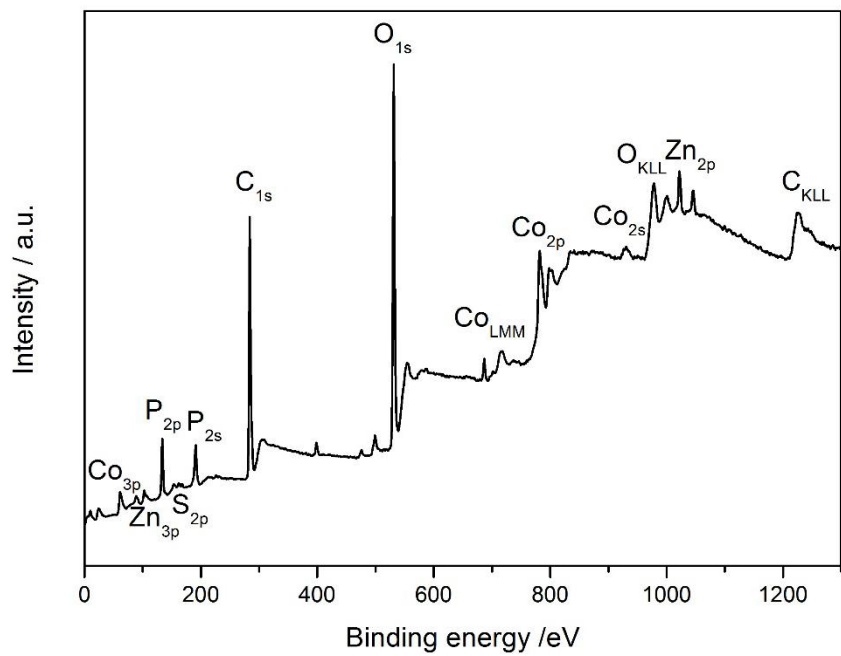


Figure S9. XPS survey spectrum of $\text{Zn}_{0.075},\text{S}-\text{Co}_{0.925}\text{P}$ NRCs/CP.

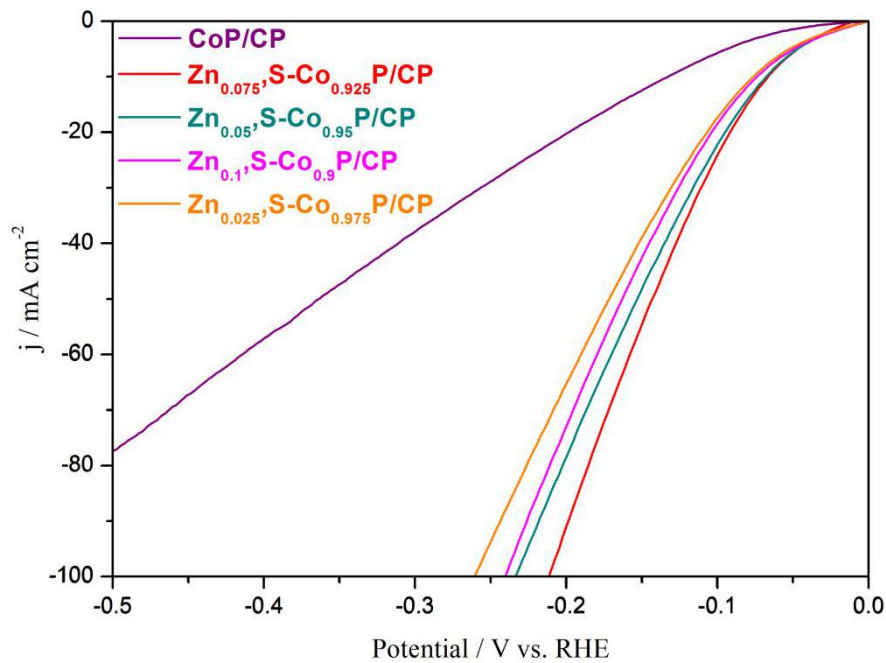


Figure S10. HER performances of the $\text{Zn}_x,\text{S}-\text{Co}_{1-x}\text{P}$ NRCs/CP ($x = 0.025, 0.05, 0.075$, and 0.1) in 1.0 M PBS.

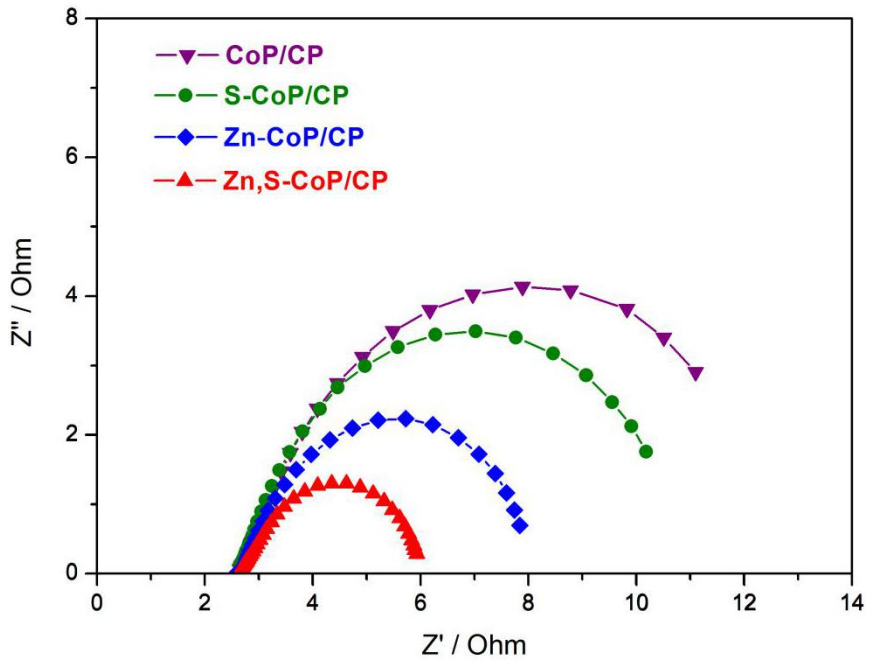


Figure S11. EIS Nyquist plots of the pure CoP, S-CoP, $\text{Zn}_{0.075}\text{-Co}_{0.925}\text{P}$, and $\text{Zn}_{0.075}\text{S-Co}_{0.925}\text{P}$ NRCs/CP for HER test in 1.0 M PBS.

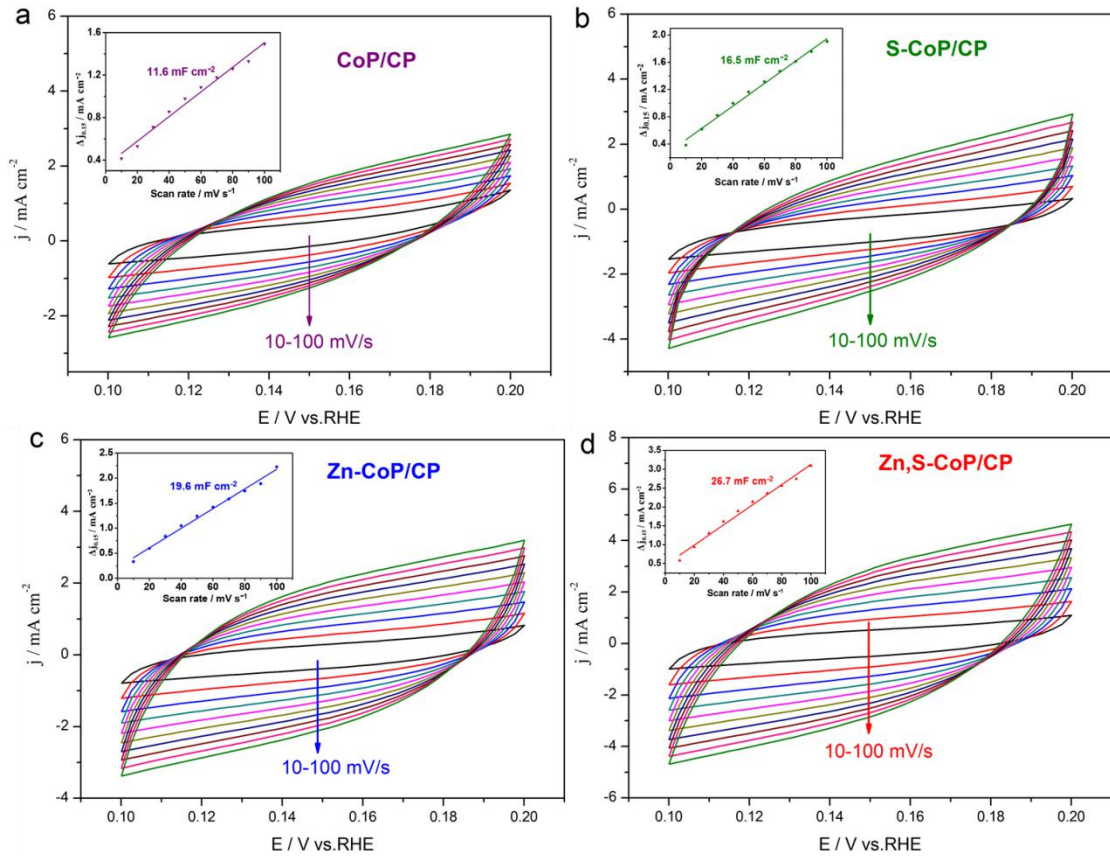


Figure S12. CVs of (a) CoP NRCs /CP, (b) S-CoP NRCs/CP, (c) Zn_{0.075}-Co_{0.925}P, and (d) Zn_{0.075},S-Co_{0.925}P NRCs/CP at different scan rates in 1.0 M PBS, and the inset is the corresponding linear fitting curves of the capacitive currents as a function of scan rates.

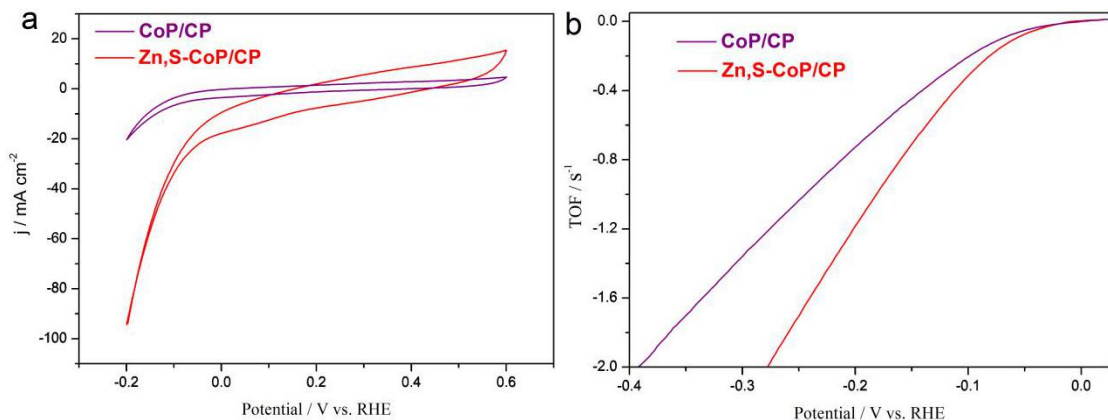


Figure S13. (a) CV curves of CoP NRCs /CP and Zn_{0.025},S-Co_{0.975}P NRCs/CP in 1.0 M PBS at a scan rate of 50 mV/s. (b) Calculated TOF of CoP NRCs/CP and Zn_{0.025},S-Co_{0.975}P NRCs/CP.

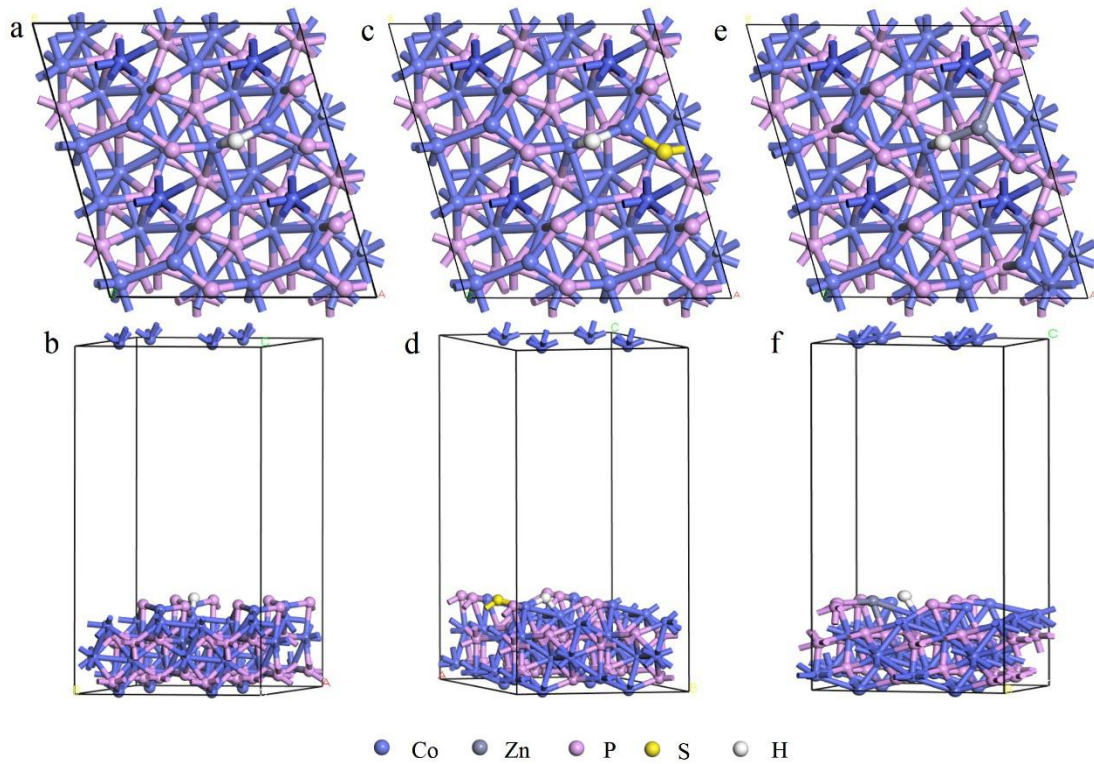


Figure S14. Top and side views of geometric configurations of H adsorption onto the (a,b) pristine CoP (111), (c,d) S-CoP (111), and (e,f) Zn-CoP (111) surfaces.

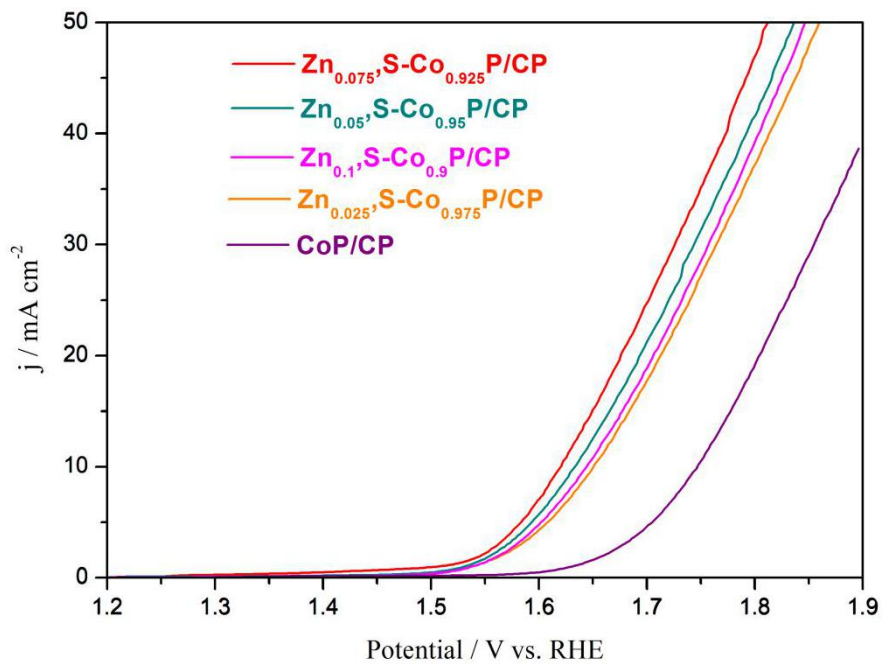


Figure S15. OER performances of the $Zn_xS\text{-Co}_{1-x}P$ NRCs/CP ($x = 0, 0.025, 0.05, 0.075$, and 0.1) in 1.0 M PBS .

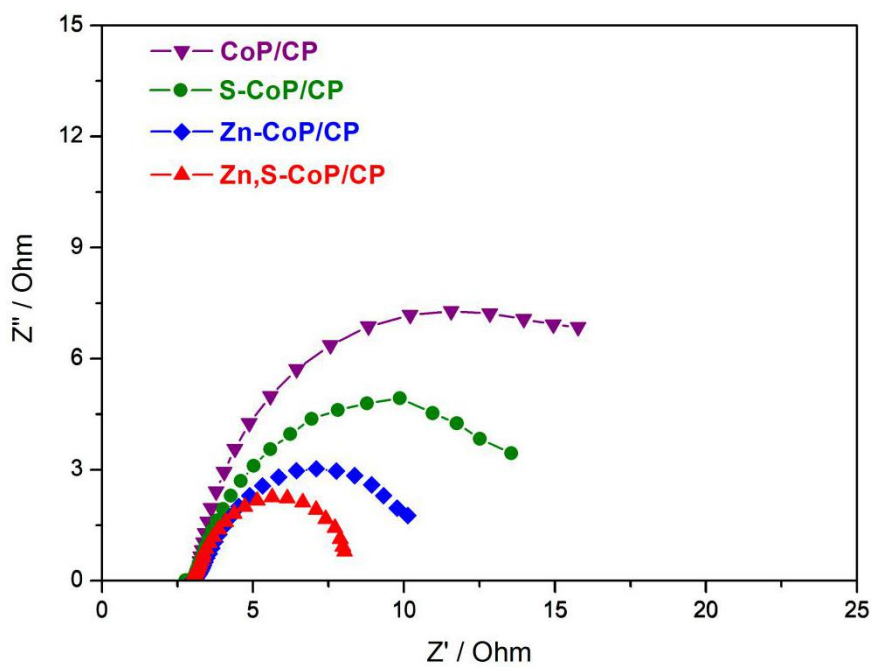


Figure S16. EIS Nyquist plots of the pure CoP , $S\text{-CoP}$, $Zn_{0.075}\text{-Co}_{0.925}P$, and $Zn_{0.075},S\text{-Co}_{0.925}P$ NRCs/CP for OER test in 1.0 M PBS .

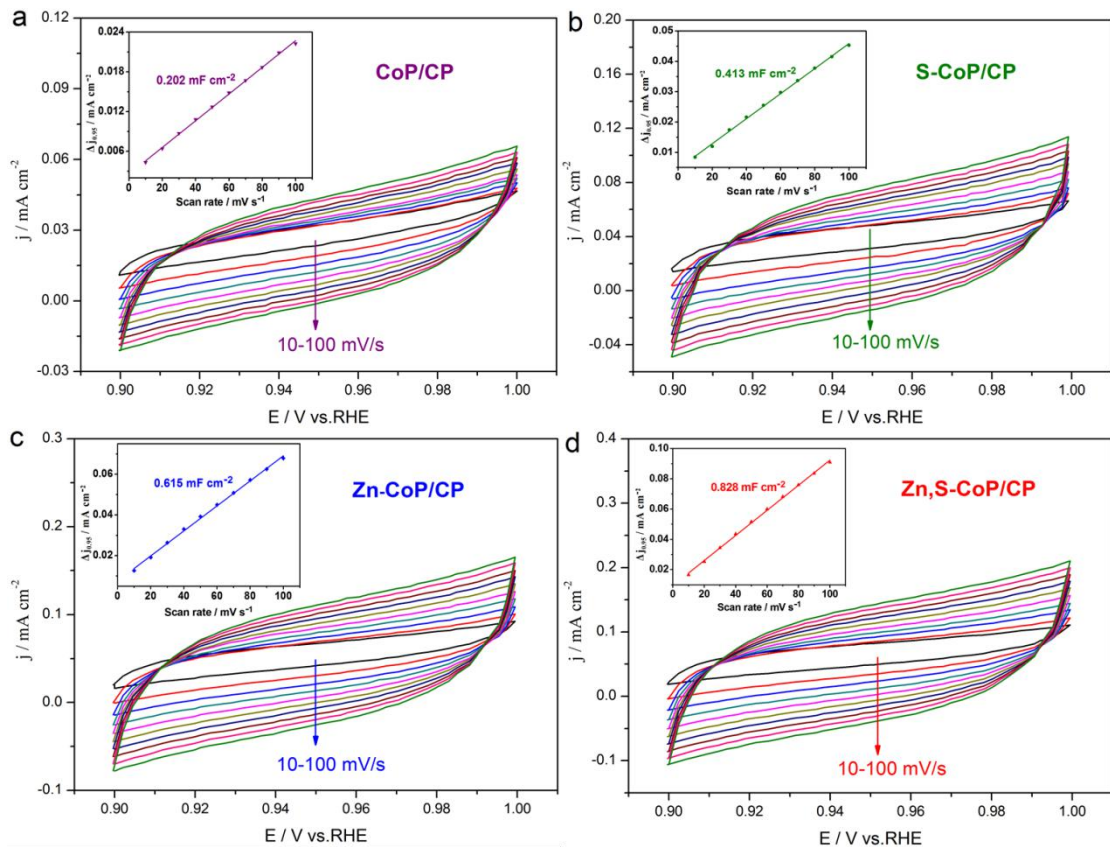


Figure S17. Electrochemical double-layer capacitance measurements at different scan rates for OER. CVs for (a) CoP NRCs /CP, (b) S-CoP NRCs/CP, (c) Zn_{0.075}-Co_{0.925}P NRCs/CP, and (d) Zn_{0.075},S-Co_{0.925}P NRCs/CP at different scan rates in 1.0 M PBS, and the inset is the corresponding linear fitting curves of the capacitive currents as a function of scan rates.

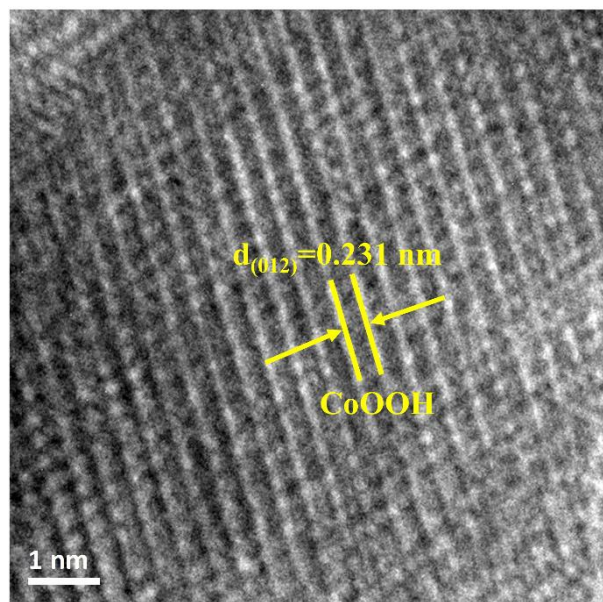


Figure S18. HRTEM image of $\text{Zn}_{0.075}\text{S}-\text{Co}_{0.925}\text{P}$ NRCs/CP after OER test in 1.0 M PBS.

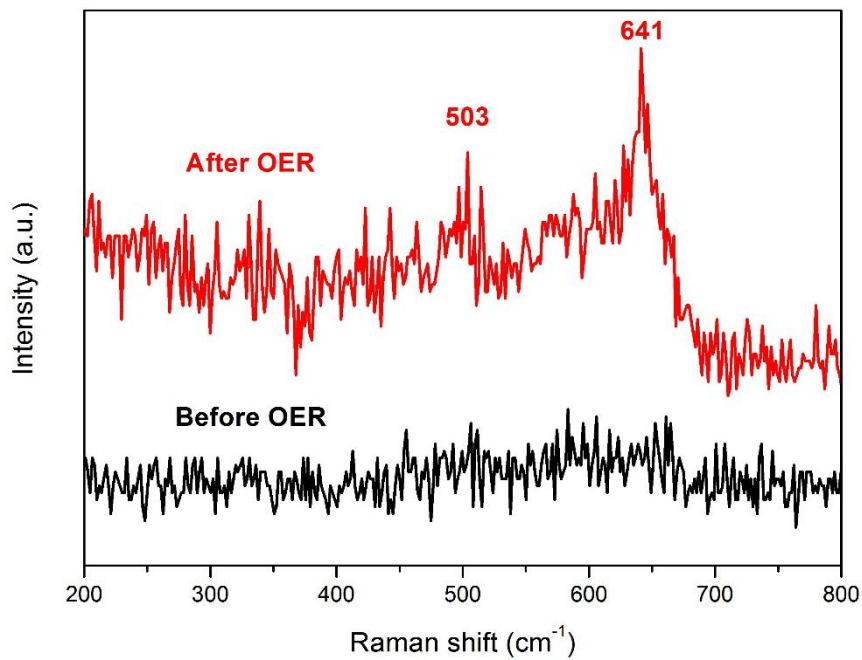


Figure S19. Raman spectra of $\text{Zn}_{0.075}\text{S}-\text{Co}_{0.925}\text{P}$ NRCs/CP before and after OER test.

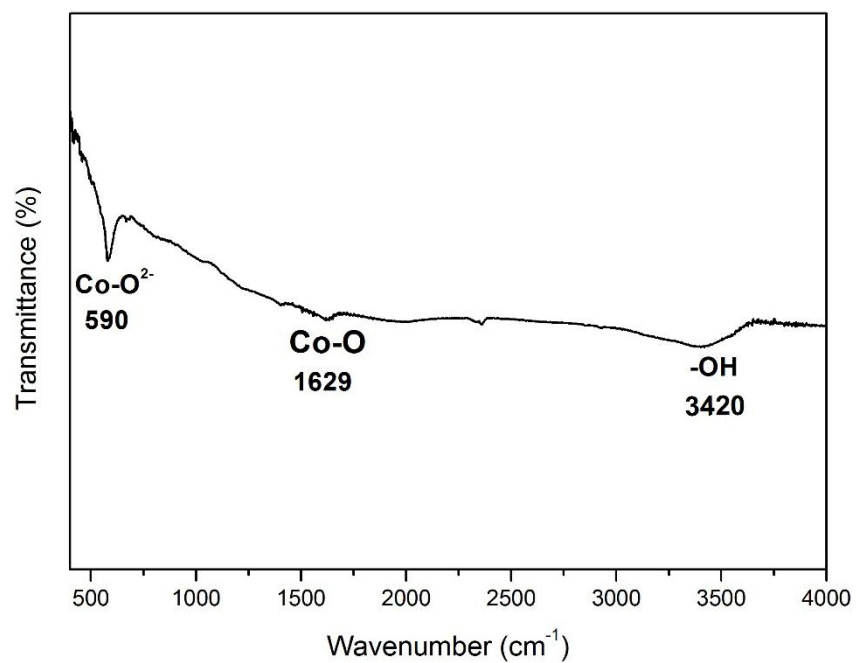


Figure S20. FTIR spectra of $\text{Zn}_{0.075}\text{S}-\text{Co}_{0.925}\text{P}$ NRCs/CP after OER test in 1.0 M PBS.

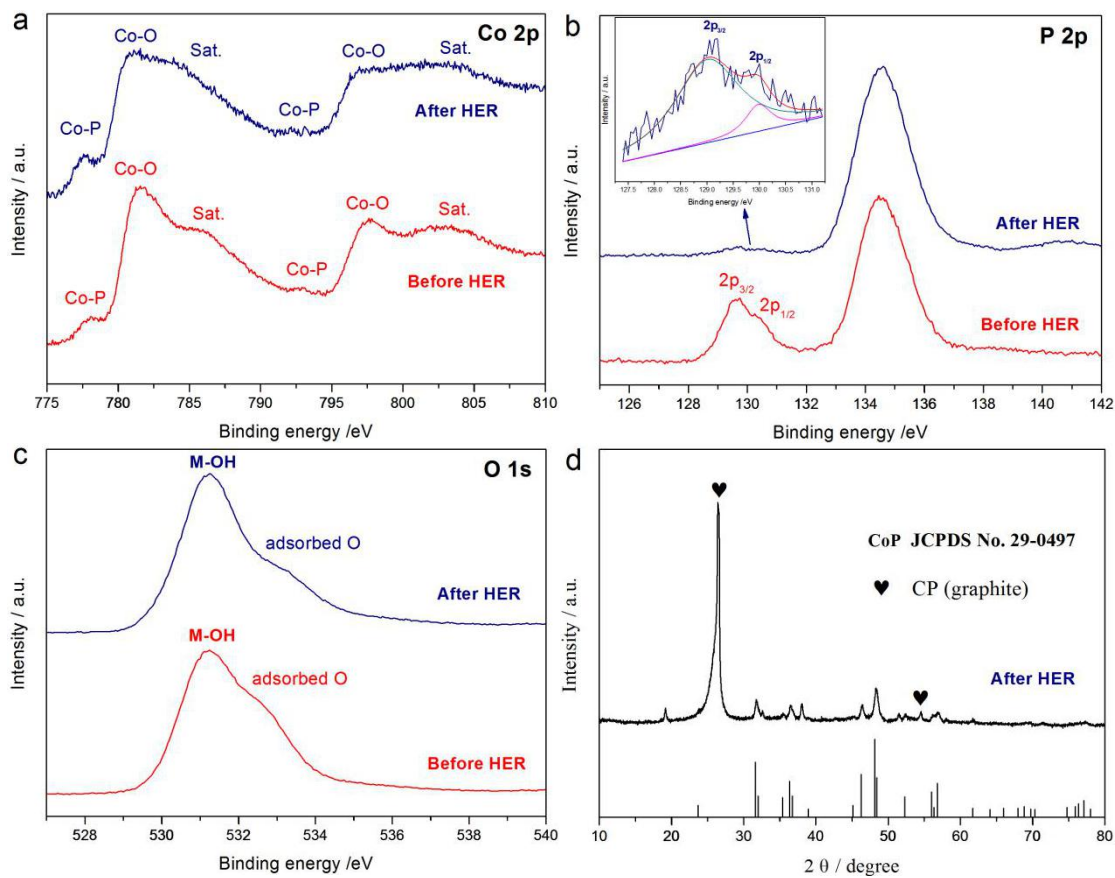


Figure S21. (a) Co 2p, (b) P 2p, and (c) O 1s XPS spectra of $\text{Zn}_{0.075}\text{S}-\text{Co}_{0.925}\text{P}$ NRCs/CP before and after HER test. (d) XRD pattern of $\text{Zn}_{0.075}\text{S}-\text{Co}_{0.925}\text{P}$ NRCs/CP after HER test.

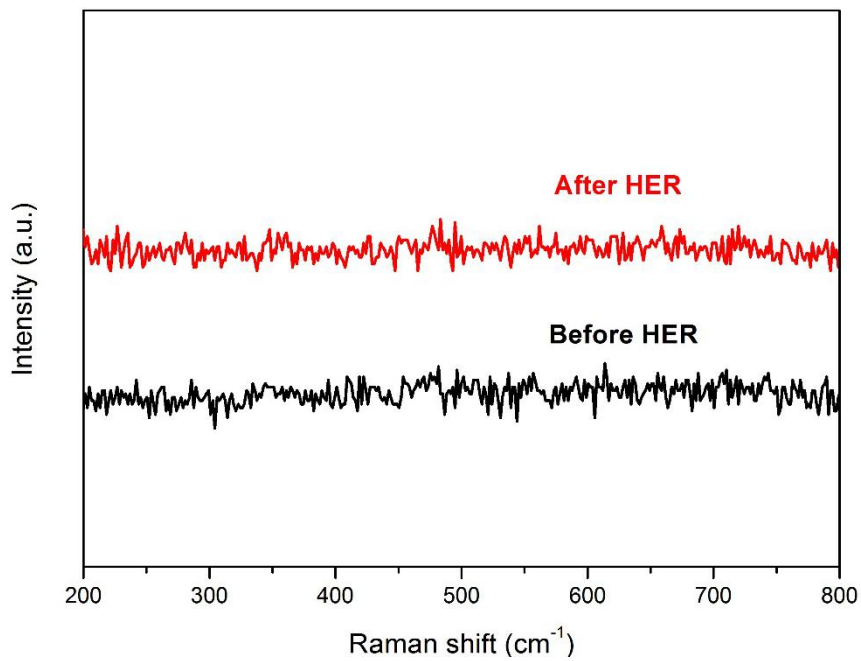


Figure S22. Raman spectra of $\text{Zn}_{0.075}\text{S}-\text{Co}_{0.925}\text{P}$ NRCs/CP before and after HER test.

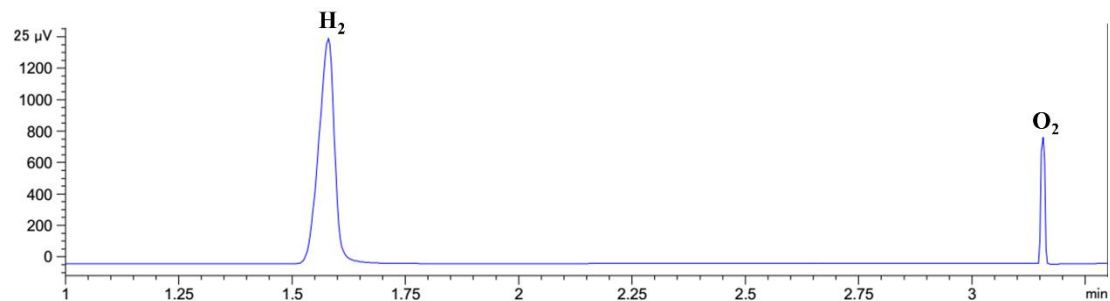


Figure S23. GC signals of the gas generated from water splitting.

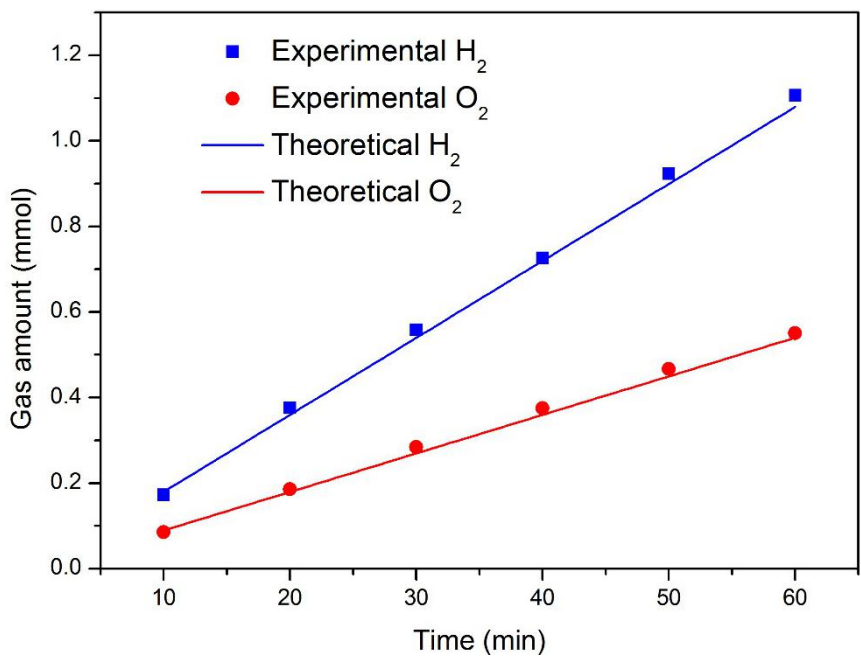


Figure S24. The amount of gas theoretical calculation and experimental measure versus time for HER and OER of $\text{Zn}_{0.075}\text{S}-\text{Co}_{0.925}\text{P}$ NRCs/CP.

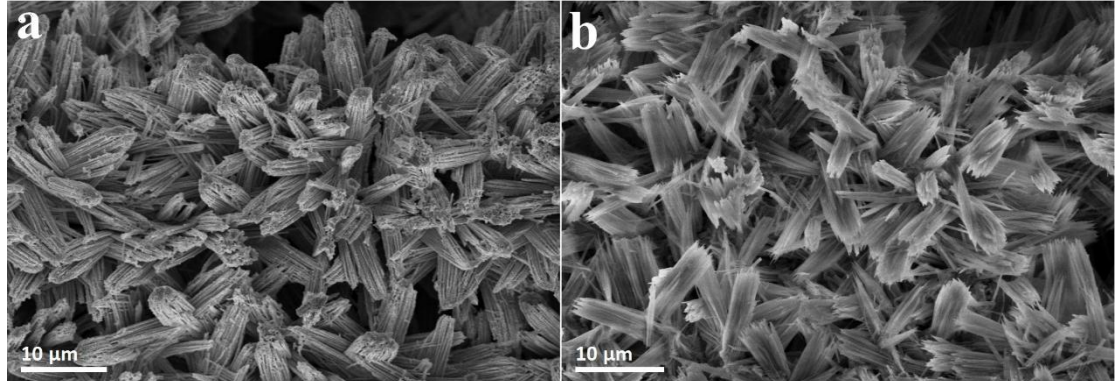


Figure S25. SEM images of the $\text{Zn}_{0.075}\text{S}-\text{Co}_{0.925}\text{P}$ NRCs/CP after (a) HER and (b) OER test.

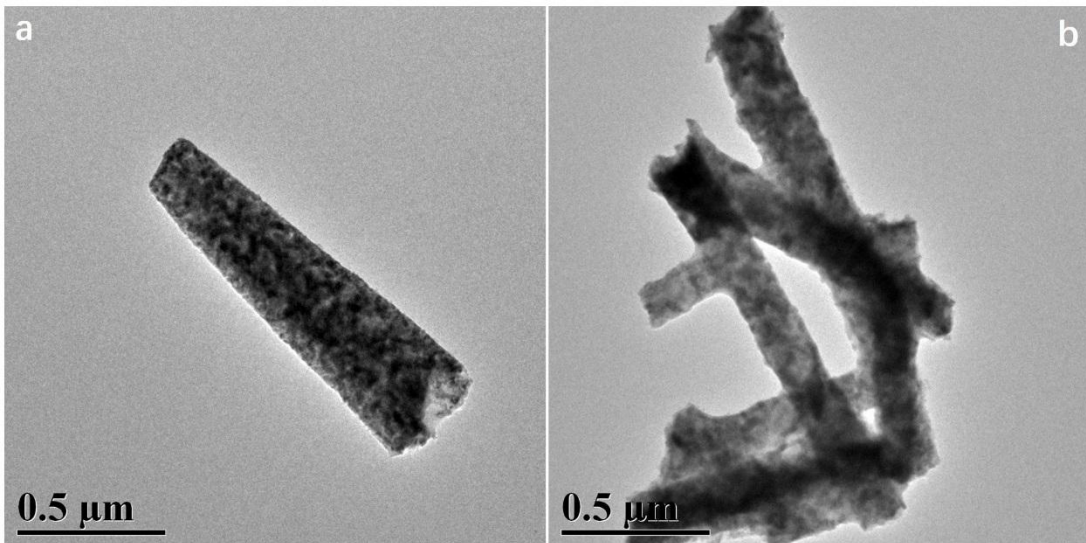


Figure S26. TEM images of the $\text{Zn}_{0.075}\text{S}-\text{Co}_{0.925}\text{P}$ NRCs/CP after (a) HER and (b) OER test.

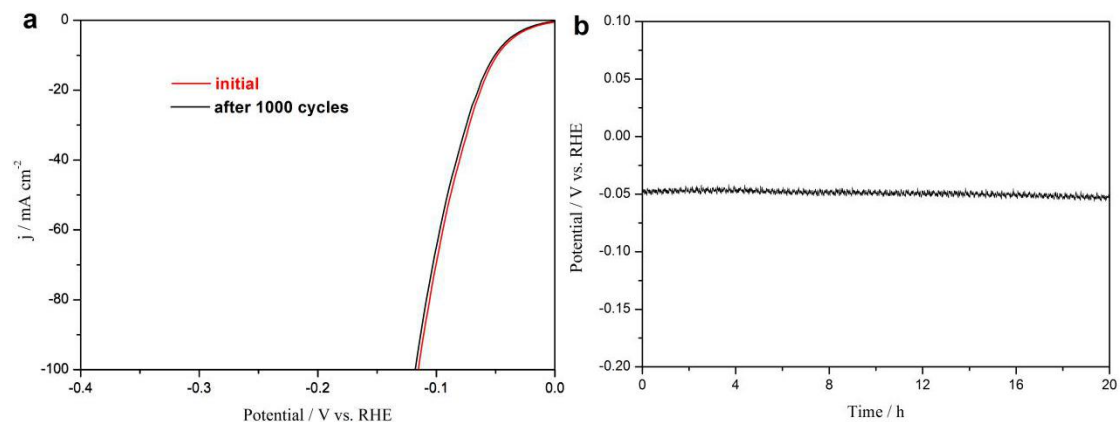


Figure S27. Alkaline HER performance. (a) LSV curves of $\text{Zn}_{0.075}\text{S}-\text{Co}_{0.925}\text{P}$ NRCs/CP before and after 1000 CV cycles. (b) Chronopotentiometry curve of $\text{Zn}_{0.075}\text{S}-\text{Co}_{0.925}\text{P}$ NRCs/CP at a constant current density of 10 mA cm^{-2} .

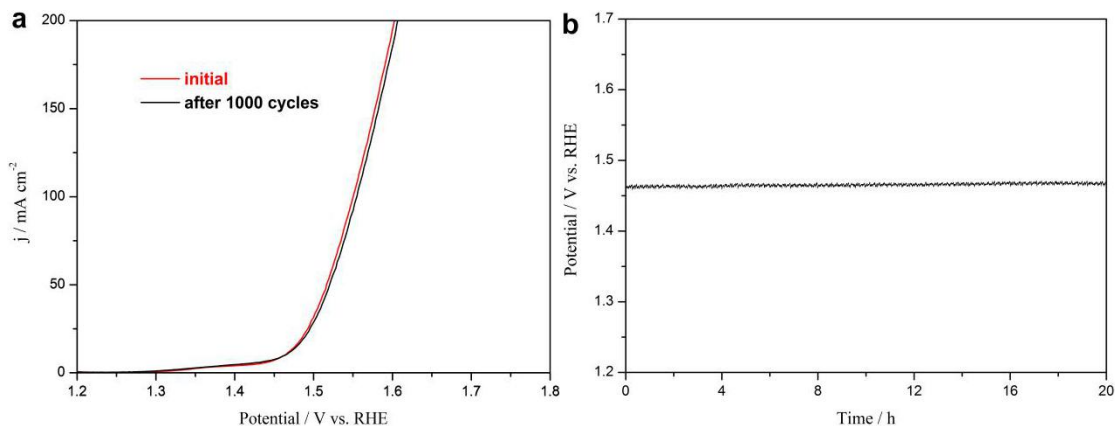


Figure S28. Alkaline OER performance. (a) LSV curves of $\text{Zn}_{0.075}\text{S-Co}_{0.925}\text{P}$ NRCs/CP before and after 1000 CV cycles. (d) Chronopotentiometry curve of $\text{Zn}_{0.075}\text{S-Co}_{0.925}\text{P}$ NRCs/CP at a constant current density of 10 mA cm^{-2} .

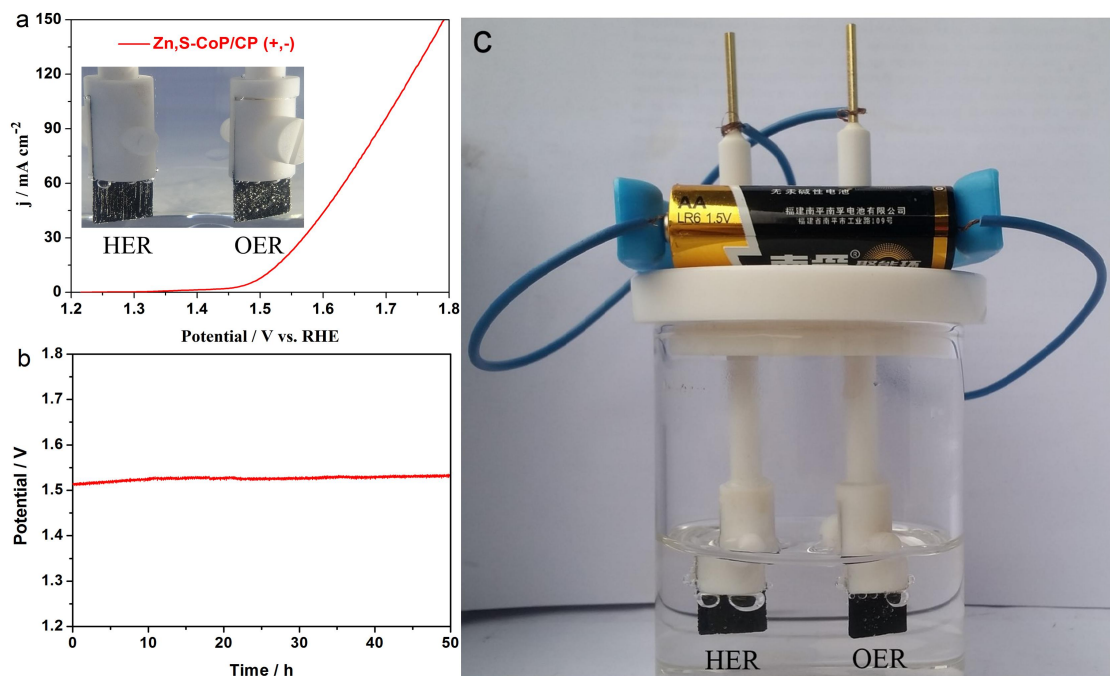


Figure S29. (a) LSV curves of $\text{Zn}_{0.075},\text{S}-\text{Co}_{0.925}\text{P}$ NRCs/CP used as both cathode and anode in a two-electrode configuration in 1.0 M KOH, and the inset is the device photograph of the two-electrode electrolyzer. (b) Chronopotentiometry curves of $\text{Zn}_{0.075},\text{S}-\text{Co}_{0.925}\text{P}$ NRCs/CP (+,-) at a constant current density of 10 mA cm^{-2} . (c) Optical image of the $\text{Zn}_{0.075},\text{S}-\text{Co}_{0.925}\text{P}$ NRCs/CP (+,-) electrolyzer powered by an AA battery and H_2 (left) and O_2 (right) bubbles formed during water electrolysis.

Table S1. ICP-OES analysis results of the element content of Zn, Co, P, and S for $\text{Zn}_x,\text{S}-\text{Co}_{1-x}\text{P}$.

Sample	Zn at%	Co at%	P at%	S at%	$\text{Zn}^{2+}/(\text{Zn}^{2+}+\text{Co}^{2+})$
CoP	0	49.81	50.19	0	0
S-CoP	0	49.86	45.20	4.94	0
$\text{Zn}_{0.075}-\text{Co}_{0.925}\text{P}$	3.69	46.18	50.13	0	0.0740
$\text{Zn}_{0.025},\text{S}-\text{Co}_{0.975}\text{P}$	1.16	48.05	45.82	4.97	0.0236
$\text{Zn}_{0.05},\text{S}-\text{Co}_{0.95}\text{P}$	2.45	47.48	45.15	4.92	0.0491
$\text{Zn}_{0.075},\text{S}-\text{Co}_{0.925}\text{P}$	3.66	45.97	45.42	4.95	0.0737
$\text{Zn}_{0.1},\text{S}-\text{Co}_{0.9}\text{P}$	4.93	44.92	45.24	4.91	0.0989

Table S2. HER performance of the Zn_{0.075}S-Co_{0.925}P NRCs/CP in this work, in comparison with other non-noble metal based catalysts in 1.0 M PBS from recent publications.

Catalysts	η (mV) at 10 mA cm ⁻²	Tafel slope mV dec ⁻¹	References
CoP/CC	106	93	<i>J. Am. Chem. Soc.</i> 2014 , <i>136</i> , 7587
CoP/Ti	149	111	<i>Chem. Mater.</i> 2014 , <i>26</i> , 4326
CoP-MNA/NF	~180*	189	<i>Adv. Funct. Mater.</i> 2015 , <i>25</i> , 7337
NiCoP/rGO	124	91	<i>Adv. Funct. Mater.</i> 2016 , <i>26</i> , 6785
Co _{0.6} Fe _{0.4} P/CNTs	105	78	<i>Adv. Funct. Mater.</i> 2017 , <i>27</i> , 1606635
Co/CoP-5	138	72.3	<i>Adv. Energy Mater.</i> 2017 , <i>7</i> , 1602355
Mn-Co-P/Ti	86	82	<i>ACS Catal.</i> 2017 , <i>7</i> , 98
NiCo ₂ P _x /CF	63	63.3	<i>Adv. Mater.</i> 2017 , <i>29</i> , 1605502
CoP@BCN-1	122	59	<i>Adv. Energy Mater.</i> 2017 , <i>7</i> , 1601671
MoP NWAs/CFP	84	63	<i>Adv. Funct. Mater.</i> 2018 , <i>28</i> , 1804600
Ni ₂ P@NPCNFs	185.3	230.3	<i>Angew. Chem. Int. Ed.</i> 2018 , <i>57</i> , 1963
PdP ₂ @CB	84.6	72.3	<i>Angew. Chem. Int. Ed.</i> 2018 , <i>57</i> , 1
Ni ₂ P@NPCNFs	185.3	230.3	<i>Angew. Chem. Int. Ed.</i> 2018 , <i>57</i> , 1963
Ni _{0.1} Co _{0.9} P/CFP	125	103	<i>Angew. Chem. Int. Ed.</i> 2018 , <i>57</i> , 15445
CoP/Co-MOF	49	63	<i>Angew. Chem. Int. Ed.</i> 2019 , <i>58</i> , 4679
CoP/NiCoP/NC	123	78	<i>Adv. Funct. Mater.</i> 2019 , <i>29</i> , 1807976
Co-Fe-P nanotubes	138	138	<i>Nano Energy</i> 2019 , <i>56</i> , 225
CoP@PC-750	85	58	<i>Small</i> 2019 , <i>15</i> , 1900550
N-Co ₂ P/CC	42	68	<i>ACS Catal.</i> 2019 , <i>9</i> , 3744
Ni-FeP/C	117	70	<i>Sci. Adv.</i> 2019 , <i>5</i> , eaav6009
Zn _{0.075} S-Co _{0.925} P/CP	67	71.6	This work

*: In 0.5 M PBS.

Table S3. OER performance of the Zn_{0.075}S-Co_{0.925}P NRCs/CP in this work, in comparison with other non-noble metal based catalysts in neutral solution from recent publications.

Catalysts	Electrolyte	η (mV) at 10 mA cm ⁻²	Tafel slope mV dec ⁻¹	References
Co-P-B/rGO	0.1 M PBS	400	68	<i>J. Mater. Chem. A</i> 2014 , <i>2</i> , 18420
Co ₃ S ₄ nanosheets	1.0 M PBS	650 mV@ 3.27 mA cm ⁻²	—	<i>Angew. Chem. Int. Ed.</i> 2015 , <i>54</i> , 11231
Mn ₅ O ₈ NPs	0.3 M PBS	580 mV@ 5 mA cm ⁻²	78.7	<i>ACS Catal.</i> 2015 , <i>5</i> , 4624
LT-LiCoO ₂	1.0 M PBS	570	75	<i>Energy Environ. Sci.</i> 2016 , <i>9</i> , 184
Ni42-300	0.1 M PBS	620	198.16	<i>Adv. Funct. Mater.</i> 2016 , <i>26</i> , 6402
Co-Bi NS/G	1.0 M PBS	570 mV@ 14.4 mA cm ⁻²	160	<i>Angew. Chem. Int. Ed.</i> 2016 , <i>55</i> , 2488
CoO/CoSe ₂ /Ti	0.5 M PBS	510	137	<i>Adv. Sci.</i> 2016 , <i>3</i> , 1500426
S-NiFe ₂ O ₄ /NF	1.0 M PBS	494	118.1	<i>Nano Energy</i> 2017 , <i>40</i> , 264
Ti@Co _{0.85} Se	1.0 M PBS	500	153	<i>Nano Energy</i> 2017 , <i>39</i> , 321
Mn-Co-Bi/CC	1.0 M PBS	366	193	<i>J. Mater. Chem. A</i> 2017 , <i>5</i> , 12091
Co-Bi/Ti	0.1 M K-Bi	469	131	<i>J. Mater. Chem. A</i> 2017 , <i>5</i> , 7305
FeNi-P/NF-A	0.1 M PBS	429	136	<i>J. Mater. Chem. A</i> 2017 , <i>5</i> , 13329
Co-Pi NA/Ti	1.0 M PBS	380	187	<i>Angew. Chem. Int. Ed.</i> 2017 , <i>56</i> , 1064
A-CoS _{4.6} O _{0.6} PNCs	0.1 M PBS	570 mV@ 4.59 mA cm ⁻²	164	<i>Angew. Chem. Int. Ed.</i> 2017 , <i>56</i> , 4858
Ni ₃ Se ₄ /Ni	1.0 M PBS	480	116	<i>ACS Appl. Mater. Interfaces</i> 2017 , <i>9</i> , 8714
Co/CoP-5	1.0 M PBS	570 mV@ 2.64 mA cm ⁻²	—	<i>Adv. Energy Mater.</i> 2017 , <i>7</i> , 1602355
Co-Se-S-O	0.1 M PBS	480	—	<i>ACS Appl. Mater. Interfaces</i> 2018 , <i>10</i> , 8231
Ni _{0.1} Co _{0.9} P-CFP	1.0 M PBS	560	133	<i>Angew. Chem. Int. Ed.</i> 2018 , <i>57</i> , 15445
CoO/Co ₄ N	1.0 M PBS	398	83	<i>J. Mater. Chem. A</i> 2018 , <i>6</i> , 24767
CoIr-0.2	1.0 M PBS	373	117.5	<i>Adv. Mater.</i> 2018 , <i>30</i> , 1707522
CoP@NPMG	1.0 M PBS	379	72	<i>Nanoscale</i> 2018 , <i>10</i> , 2603
NC-CNT/CoP-N	1.0 M PBS	420	—	<i>J. Mater. Chem. A</i> 2018 , <i>6</i> , 9009
np-Co ₉ S ₄ P ₄	1.0 M PBS	570 mV@ 25.9 mA cm ⁻²	106	<i>ACS Appl. Mater. Interfaces</i> 2019 , <i>11</i> , 3880
Ni(S _{0.5} Se _{0.5}) ₂	1.0 M PBS	501	94	<i>J. Mater. Chem. A</i> 2019 , <i>7</i> , 16793
Zn _x S-CoP/CP	1.0 M PBS	391	99.7	This work

Table S4. Comparison of overall water-splitting performance of Zn_{0.075}S-Co_{0.925}P

NRCs/CP and other non-noble metal bifunctional electrocatalysts in neutral media.

Catalysts	Electrolyte	E (V)@10 mA cm ⁻²	References
CoO/CoSe ₂ -Ti	0.5 M PBS	2.18	<i>Adv. Sci.</i> 2016 , <i>3</i> , 1500426
CoP NA/CC	1.0 M PBS	1.6 @ 2 mA cm ⁻²	<i>ChemElectroChem</i> 2017 , <i>4</i> , 1840
S-NiFe ₂ O ₄ /NF	1.0 M PBS	1.95	<i>Nano Energy</i> 2017 , <i>40</i> , 264
Fe-CoP/CC	0.1 M K-Bi	1.95	<i>ChemSusChem</i> 2017 , <i>10</i> , 3188
CoO/Co ₄ N	1.0 M PBS	1.79	<i>J. Mater. Chem. A</i> 2018 , <i>6</i> , 24767
CoP@NPMG	1.0 M PBS	1.74	<i>Nanoscale</i> 2018 , <i>10</i> , 2603
Ni _{0.1} Co _{0.9} P/CP	1.0 M PBS	1.89	<i>Angew. Chem. Int. Ed.</i> 2018 , <i>57</i> , 15445
PdP ₂ @CB	1.0 M PBS	1.59	<i>Angew. Chem. Int. Ed.</i> 2018 , <i>57</i> , 1
NC-CNT/CoP-N	1.0 M PBS	1.69	<i>J. Mater. Chem. A</i> 2018 , <i>6</i> , 9009
Ni(S _{0.5} Se _{0.5}) ₂	1.0 M PBS	1.87	<i>J. Mater. Chem. A</i> 2019 , <i>7</i> , 16793
CoMnNiS-NF-31	1.0 M PBS	1.80	<i>J. Am. Chem. Soc.</i> 2019 , <i>141</i> , 10417
v-CoFe LDH	1.0 M PBS	1.76	<i>ACS Energy Lett.</i> 2019 , <i>4</i> , 1412
Zn _x S-CoP/CP	1.0 M PBS	1.70	This work

Table S5. HER performance of the Zn_{0.075}S-Co_{0.925}P NRCs/CP in this work, in comparison with other non-noble metal based catalysts in 1.0 M KOH from recent publications.

Catalysts	η (mV) at 10 mA cm ⁻²	Tafel slope mV dec ⁻¹	References
CoP/CC	209	129	<i>J. Am. Chem. Soc.</i> 2014 , <i>136</i> , 7587
Co-P film	94	42	<i>Angew. Chem. Int. Ed.</i> 2015 , <i>54</i> , 6251
CoP NS/C	111	70.9	<i>Green Chem.</i> 2016 , <i>18</i> , 2287
CoNiP@NF	155	113	<i>J. Mater. Chem. A</i> 2016 , <i>4</i> , 10195
np-(Co _{0.52} Fe _{0.48}) ₂ P	79	40	<i>Energy Environ. Sci.</i> 2016 , <i>9</i> , 2257
Ni _{0.51} Co _{0.49} P film	82	43	<i>Adv. Funct. Mater.</i> 2016 , <i>26</i> , 7644
CoP@NC	129	58	<i>ACS Catal.</i> 2017 , <i>7</i> , 3824
Mn-Co-P/Ti	76	52	<i>ACS Catal.</i> 2017 , <i>7</i> , 98
Ce-CoP NWs/Ti	92	63.5	<i>Nano Energy</i> 2017 , <i>38</i> , 290
Fe-CoP/Ti	78	75	<i>Adv. Mater.</i> 2017 , <i>29</i> , 1602441
CoMoP@C	81	55.5	<i>Energy Environ. Sci.</i> 2017 , <i>10</i> , 788
Ni-Co-P HNBs	107	46	<i>Energy Environ. Sci.</i> 2018 , <i>11</i> , 872
Co _{0.93} Ni _{0.07} P ₃ /CC	87	60.7	<i>ACS Energy Lett.</i> 2018 , <i>3</i> , 1744
CoP/NCNHP	115	66	<i>J. Am. Chem. Soc.</i> 2018 , <i>140</i> , 2610
CoP@3D MXene	168	58	<i>ACS Nano</i> 2018 , <i>12</i> , 8017
Co-Fe-P nanotubes	86	66	<i>Nano Energy</i> 2019 , <i>56</i> , 225
Ni-CoP/HPFs	92	71	<i>Nano Energy</i> 2019 , <i>56</i> , 411
Co-P@PC-750	76	52	<i>Small</i> 2019 , <i>15</i> , 1900550
Er-doped CoP	66	61	<i>J. Mater. Chem. A</i> 2019 , <i>7</i> , 5769
N-Co ₂ P/CC	34	51	<i>ACS Catal.</i> 2019 , <i>9</i> , 3744
CoP/Co-MOF	34	56	<i>Angew. Chem. Int. Ed.</i> 2019 , <i>58</i> , 4679
CoP/NiCoP/NC	75	64	<i>Adv. Funct. Mater.</i> 2019 , <i>29</i> , 1807976
Zn _{0.075} S-Co _{0.925} P/CP	49	41.5	This work

Table S6. OER performance of the Zn_{0.075}S-Co_{0.925}P NRCs/CP in this work, in comparison with other non-noble metal based catalysts in 1.0 M KOH from recent publications.

Catalysts	η (mV) at 10 mA cm ⁻²	Tafel slope mV dec ⁻¹	References
CoP-MNA/NF	290	65	<i>Adv. Funct. Mater.</i> 2015 , <i>25</i> , 7337
Co-P film	345	47	<i>Angew. Chem. Int. Ed.</i> 2015 , <i>54</i> , 6251
CoP NR/C	320	71	<i>ACS Catal.</i> 2015 , <i>5</i> , 6874
np-(Co _{0.52} Fe _{0.48}) ₂ P	270	30	<i>Energy Environ. Sci.</i> 2016 , <i>9</i> , 2257
NiCoP/NF	280	87	<i>Nano Lett.</i> 2016 , <i>16</i> , 7718
CoMnP nanoparticles	330	61	<i>J. Am. Chem. Soc.</i> 2016 , <i>138</i> , 4006
CoP/rGO	340	66	<i>Chem. Sci.</i> 2016 , <i>7</i> , 1690
CoP NS/C	277	85.6	<i>Green Chem.</i> 2016 , <i>18</i> , 2287
NiCoP/Ti	310	52	<i>Adv. Mater. Interfaces</i> 2016 , <i>3</i> , 1500454
NiCoP/C	330	96	<i>Angew. Chem. Int. Ed.</i> 2017 , <i>56</i> , 3897
Fe-CoP/Ti	230	67	<i>Adv. Mater.</i> 2017 , <i>29</i> , 1602441
Ni-Co-P HNBs	270	76	<i>Energy Environ. Sci.</i> 2018 , <i>11</i> , 872
Mo-CoOOH/CC	305	56	<i>Nano Energy</i> 2018 , <i>48</i> , 73
S:CoP@NG	260	108	<i>Nano Energy</i> 2018 , <i>53</i> , 286
CoP/NCNHP	310	70	<i>J. Am. Chem. Soc.</i> 2018 , <i>140</i> , 2610
CoP@3D MXene	290	51	<i>ACS Nano</i> 2018 , <i>12</i> , 8017
S:Co ₂ P@CC	290	82	<i>Chem. Mater.</i> 2018 , <i>30</i> , 8861
CoP@NPMG	276	54	<i>Nanoscale</i> , 2018 , <i>10</i> , 2603
Co-P@PC-750	283	53	<i>Small</i> 2019 , <i>15</i> , 1900550
NieCoP@C	279	54	<i>Nano Energy</i> 2019 , <i>62</i> , 136
Mo ₅₁ Ni ₄₀ Fe ₉ NBs	257	51	<i>ACS Catal.</i> 2019 , <i>9</i> , 1013
Er-doped CoP	256	70	<i>J. Mater. Chem. A</i> 2019 , <i>7</i> , 5769
Cr-FeNiP/NCN	240	72.36	<i>Adv. Mater.</i> 2019 , <i>31</i> , 1900178
Zn _{0.075} S-Co _{0.925} P/CP	233	71.7	This work

Table S7. Summary of recent reported representative of bifunctional non-noble metal based catalysts for overall water-splitting in 1.0 M KOH.

Catalysts	Potential (V) at 10 mA cm ⁻²	References
Co-P film	1.65	<i>Angew. Chem. Int. Ed.</i> 2015 , <i>54</i> , 6251
CoP-MNA	1.62	<i>Adv. Funct. Mater.</i> 2015 , <i>25</i> , 7337
CoP NR	1.587	<i>ACS Catal.</i> 2015 , <i>5</i> , 6874
np-(Co _{0.52} Fe _{0.48}) ₂ P	1.53	<i>Energy Environ. Sci.</i> 2016 , <i>9</i> , 2257
NiCoP/Ti	1.64	<i>Adv. Mater. Interfaces</i> 2016 , <i>3</i> , 1500454
CoP/GO	1.7	<i>Chem. Sci.</i> 2016 , <i>7</i> , 1690
NiCoP/NF	1.58	<i>Nano Lett.</i> 2016 , <i>16</i> , 7718
Fe-CoP/Ti	1.60	<i>Adv. Mater.</i> 2017 , <i>29</i> , 1602441
Co ₄ Ni ₁ P NTs	1.59	<i>Adv. Funct. Mater.</i> 2017 , <i>27</i> , 1703455
Ni-Co-P HNBs	1.62	<i>Energy Environ. Sci.</i> 2018 , <i>11</i> , 872
Mo-CoP/CC	1.56	<i>Nano Energy</i> 2018 , <i>48</i> , 73
S:CoP@NF	1.617	<i>Nano Energy</i> 2018 , <i>53</i> , 286
CoP/NCNHP	1.64	<i>J. Am. Chem. Soc.</i> 2018 , <i>140</i> , 2610
Co-P@PC-750	1.60	<i>Small</i> 2019 , <i>15</i> , 1900550
Er-doped CoP	1.58	<i>J. Mater. Chem. A</i> 2019 , <i>7</i> , 5769
Co@N-CS/N-HCP@CC	1.545	<i>Adv. Energy Mater.</i> 2019 , <i>9</i> , 1803918
NiFeP/SG	1.54	<i>Nano Energy</i> 2019 , <i>58</i> , 870
CoP@NiFe-OH/SPNF	1.53	<i>Nano Energy</i> 2019 , <i>63</i> , 103821
Co ₃ S ₄ /EC-MOF	1.55	<i>Adv. Mater.</i> 2019 , <i>31</i> , 1806672
Ni,Zn-CoO NRs	1.52	<i>Adv. Mater.</i> 2019 , <i>31</i> , 1807771
Cr-doped FeNi-P/NCN	1.50	<i>Adv. Mater.</i> 2019 , <i>31</i> , 1900178
Zn _{0.075} S-Co _{0.925} P/CP	1.51	This work